Low-frequency subthalamic neural oscillations are involved in explicit and implicit facial emotional processing - a local field potential study

Abbreviated title: Subthalamic LFP during implicit facial emotional processing

Thibaut Dondaine[1]*, Joan Duprez[2]*, Jean-François Houvenaghel[3,4], Julien Modolo[2], Claire Haegelen[2,5], Gabriel Robert[3,6], Bruno Millet[7], Dominique Drapier[3,6], Marc Vérin[3,4], Paul Sauleau[3,8]

* Co-first authors (equally contributed)

[1] Univ. Lille, Inserm, CHU Lille, U1172 - LilNCog - Lille Neuroscience & Cognition, F-59000 Lille, France

[2] Univ Rennes, INSERM, LTSI - UMR 1099, F-35000 Rennes, France

[3] 'Behavior and Basal Ganglia' research unit (EA 4712), University of Rennes 1, 2 Avenue Léon Bernard, 35043 Rennes, France

[4] Neurology department, Rennes University Hospital, 2 Rue Henri Le Guilloux, 35033, Rennes, Cedex 9, France

[5] Neurosurgery department, Rennes University Hospital, 2 Rue Henri Le Guilloux, 35033, Rennes, Cedex 9, France

[6] Psychiatry Department, Rennes University Hospital, 108 avenue du Général Leclerc, 35703 Rennes, France

[7]Psychiatry Department, Pitié-Salpêtrière Hospital, Paris, France

[8]Neurophysiology department, Rennes University Hospital, 2 Rue Henri Le Guilloux, 35033, Rennes, Cedex 9, France

Corresponding author:
Joan Duprez
joan.duprez@univ-rennes1.fr
Inserm, LTSI [(Laboratoire Traitement du Signal et de l'Image)] - UMR 1099, SESAME team
Université de Rennes 1, Campus de Beaulieu, Bât 22 bureau 512
35042 Rennes – Cedex - France

Declarations of interest: none

Funding: The study funded by PHRC-IR grant no. IDRCB: 2011-A00392-39. The funders had no role in data collection, discussion of content, preparation of the manuscript, or decision to publish.

Acknowledgements: The authors would like to thank all the patients who took part in this study. We are also grateful to Didier Grandjean and Christophe Mermoud for his help in setting up the acquisition system.

Abstract

In addition to the subthalamic nucleus' (STN) role in motricity, STN deep brain stimulation (DBS) for Parkinson's disease (PD) has also uncovered its involvement in cognitive and limbic processing. STN neural oscillations analyzed through local field potential (LFP) recordings have been shown to contribute to emotional (mostly in the alpha band [8-12 Hz]) and cognitive processing (theta [4-7 Hz] and beta [13-30 Hz] bands). In this study, we aimed at testing the hypothesis that STN oscillatory activity is involved in explicit and implicit processing of emotions. We used a task that presented the patients with emotional facial expressions and manipulated the cognitive demand by either asking them to identify the emotion (explicit task) or the gender of the face (implicit task). We evaluated emotion and task effects on STN neural oscillations power and inter-trial phase consistency. Our results revealed that STN delta power was influenced by emotional valence, but only in the implicit task. Interestingly, the strongest results were found for inter-trial phase consistency: we found an increased consistency for delta oscillations in the implicit task as compared to the explicit task. Furthermore, increased delta and theta consistency were associated with better task performance. These low-frequency effects are similar to the oscillatory dynamics described during cognitive control. We interpret these findings as reflecting a greater need for cognitive control. Overall, our study suggests that low-frequency STN neural oscillations, especially their functional organization, are involved in implicit emotional processing.

Highlights:

- STN LFPs were recorded during an emotional/gender recognition task in PD patients
- STN delta power increase depended on emotional valence in the implicit task only
- STN delta inter-trial phase consistency increase was greater for the implicit task
- Delta/theta inter-trial phase consistency was associated with task accuracy
- The STN is involved in the interaction between emotional and cognitive processing

Keywords: Subthalamic nucleus; Local field potential; Neural oscillations; Emotion; Facial expression; Parkinson's disease

Abbreviations: DBS, deep brain stimulation; ITPC, inter-trial phase clustering; LFP, Local Field Potential; PD, Parkinson's disease; STN, subthalamic nucleus; UPDRS, Unified Parkinson's Disease Rating Scale; S&E, Schwab & England; H&Y, Hoehn & Yahr; LEDD, levodopa-equivalent daily dose; MDRS, Mattis Dementia Rating Scale.

1. Introduction

Deep brain stimulation (DBS) of the subthalamic nucleus (STN) is a well-recognized neurosurgical treatment for advanced Parkinson's disease (PD). Aside from its beneficial, therapeutic effects on motor symptoms, STN-DBS has also been associated with detrimental cognitive (Elgebaly et al., 2018; Odekerken et al., 2015) and emotional effects (Péron et al., 2012). For instance, some studies have pointed out a deficit of facial emotion recognition following STN-DBS (Biseul et al., 2005; Drapier et al., 2008; Dujardin et al., 2004; Schroeder et al., 2004). The STN is divided in motor, associative and limbic territories (Plantinga et al., 2018), and because of its anatomical and functional location, it maintains links with many cerebral regions involved in the processing of cognitive and emotional information.

The different roles of the STN have also been supported by the investigation of its electrical activity through local field potential (LFP) recordings, which allow a direct measurement of the nucleus activity. These are performed using the DBS electrodes for recordings during the time period between electrode implantation and subcutaneous stimulator implantation. LFP recordings during task completion allowed to investigate STN electrical activity, notably in the time-frequency domain, which describes the dynamics of neural oscillations involved in different situations and frequencies. For instance, abnormal motor activity has been associated with increased STN beta (13-30 Hz) oscillations power (Kühn et al., 2005; Little and Brown, 2014). Regarding cognitive functioning, situations of greater cognitive control are associated with a systematic increase in STN theta (4-7 Hz) power (Duprez et al., 2019; Zavala et al., 2015), and top-down attentional mobilization for relevant information was linked with increased beta power (Engel and Fries, 2010; Zavala et al., 2015).

Regarding emotional processing, a decrease in alpha (8-12 Hz) power followed passive viewing of emotional pictures (Brücke et al., 2007; Kühn et al., 2005) and was further shown to be modulated by depressive symptoms (Huebl et al., 2011). The STN appears to have a specific role in the processing of valence of emotional stimuli, since pleasant pictures (as compared to unpleasant pictures) are associated with a decrease in alpha power (Brücke et al., 2007; Huebl et al., 2014). STN involvement in arousal induced by emotional pictures is more nuanced, with reports of both arousal-specific activity (Sieger et al., 2015) and absence of it (Brücke et al., 2007). All these studies have pointed out the involvement of STN neural oscillations, especially in the alpha band, in visual emotional processing. However, none of them have specifically focused on STN activity during emotional face recognition, since facial stimuli have been often merged with many emotional stimuli of various natures.

Emotion and cognition, although relating to different concepts, are not easily separable in terms of behavior and neural substrates, and are in constant interaction (Dolan, 2002; Ochsner and Phelps, 2007; Pessoa, 2008). Human faces carry relevant biological and social signals which should be processed rapidly to adapt behavior. Given the functional overlapping territories of the STN and its role in integrating motor, cognitive, and emotional information, this nucleus is ideally located to participate in the interaction between emotion and cognition. One method to assess this interaction relies on contrasting the activity of the structure between explicit and implicit emotional tasks (Carretié, 2014; Cohen et al., 2016). In explicit tasks, attention is allocated to emotion recognition, while in implicit tasks attention is oriented towards another characteristic of the stimulus (e.g., gender). While the aforementioned studies have shown that the STN is involved in explicit emotional recognition,

there is still no electrophysiological study focusing on facial emotion recognition and considering the involvement of the STN in implicit emotional processing.

In order to evaluate the STN's role in implicit emotional processing, we have recorded LFPs from the STN during a task based on emotional faces recognition, in which we modulated attention orientation using implicit (gender task) and explicit (emotional discrimination task) instructions. We expected to observe an activity differentially modulated by emotional valence (neutral *versus* negative emotion) and attention orientation (implicit *versus* explicit task). Since both emotional- and cognitive-related activity were expected, several frequencies were hypothesized to be modulated during the task, especially in the theta, alpha and beta bands. Furthermore, we aimed at investigating for the first time the synchronization of the STN neural oscillations across trials, and whether this synchronization is modulated by task factors. Finally, we investigated STN-behavior relationships through the evaluation of associations between time-frequency dynamics and task performance.

2. Methods

2.1. Patients and surgery

Sixteen patients with idiopathic PD undergoing bilateral STN DBS at Rennes University hospital took part in this study (N=16, 9 women). This patient group is the same as in (Duprez et al., 2019), but focusing on a different cognitive task. Patients underwent STN DBS following disabling motor symptoms uncontrolled by optimal pharmacological therapy, and were selected following standard criteria (Welter et al., 2002). Neuropsychological testing (described in details in Péron et al., 2017) indicated that patients were free from major attentional or executive disorders and did not have deficits in face recognition as estimated with the Benton facial recognition test (Benton et al., 1994). Patients' clinical characteristics are presented in Table 1.

Table 1: *Patients' preoperative clinical characteristics (average ± standard deviation).*

N	14
Age (years)	52.6 ± 7.1
Education level (years)	12.5 ± 3.4
Sex (F/M)	7/7
Disease lateralization (R/L)	8/6
Disease duration (years)	9.4 ± 2.4
UPDRS-III ON dopa	10.6 ± 7.5

UPDRS-III OFF dopa	32.3 ± 5.4
S&E ON dopa (%)	84.6 ± 13.9
S&E OFF dopa (%)	69.2 ± 20.2
H&Y ON dopa	1 ± 1
H&Y OFF dopa	2.3 ± 0.7
LEDD at the time of recording (mg/day)	800.8 ± 378.4
MDRS (/144)	140.8 ± 3.1
Benton face recognition test	44.7 ± 3.4

Abbreviations: *F: female; M: male; R: right; L: left; UPDRS: Unified Parkinson's Disease Rating Scale; S&E: Schwab & England; H&Y: Hoehn & Yahr; LEDD: levodopa-equivalent daily dose; MDRS: Mattis Dementia Rating Scale.*

Surgery was performed under local anesthesia, using MRI determination of the target, intraoperative microrecordings and assessment of the clinical effects of stimulation. Electrodes with four platinum-iridium cylindrical surfaces (1.27 mm in diameter, 1.5 mm in length, contact-to-contact separation of 0.5 mm; 3389; Medtronic, Minneapolis, MN, USA) were implanted bilaterally in all patients. Implantation was performed so that the lowest contact was positioned at the level of the STN ventral border to use the above contacts to stimulate the sensorimotor part of the nucleus, or at the interface between the subthalamic region and the zona incerta. The first contact (contact 0) was the most ventral, and the fourth

(contact 3) was the most dorsal. Correct electrodes position was verified post-operatively using a 3D CT brain scan.

This study was conducted in accordance with the declaration of Helsinki, and was approved by the Rennes University Hospital ethics committee (approval number IDRCB: 2011-A00392-39). All patients gave their informed written consent after a thorough description of the study. Two patients were excluded from further behavioral and LFP analyses as a result of artifacted data (see section 3.2.1).

2.2. Experimental task

The test consisted of two tasks always presented in the same order, which differed by the focus of attention (gender vs. emotion). The first task was an implicit emotional task (with a gender categorization), and the second task was an explicit emotional task (with an emotional labeling). For the implicit emotional task, although faces could express fear or a neutral expression (which was not specified to patients), patients were instructed to answer the question “Did the face represent a man or a woman?” by pressing with their left/right index a left/right button figuring the indication “Man” or “Woman”. For the explicit emotional task, patients were instructed to answer the question “Did the face display fear or a neutral expression?” by pressing with their left/right index a left/right button figuring the indication “Fear” or “Neutral”. We used a set of 80 colored pictures adapted from the Karolinska Directed Emotional Faces database with 20 men and 20 women (Lundqvist et al., 1998) displaying two emotional expressions (fearful or neutral). Non-facial features (hair, neck and clothes) were removed by applying a 250 x 350 pixel elliptical mask. Since these parameters were not controlled in the original version, the luminance and spatial frequencies of each stimulus were normalized using Matlab (Delplanque et al., 2007).

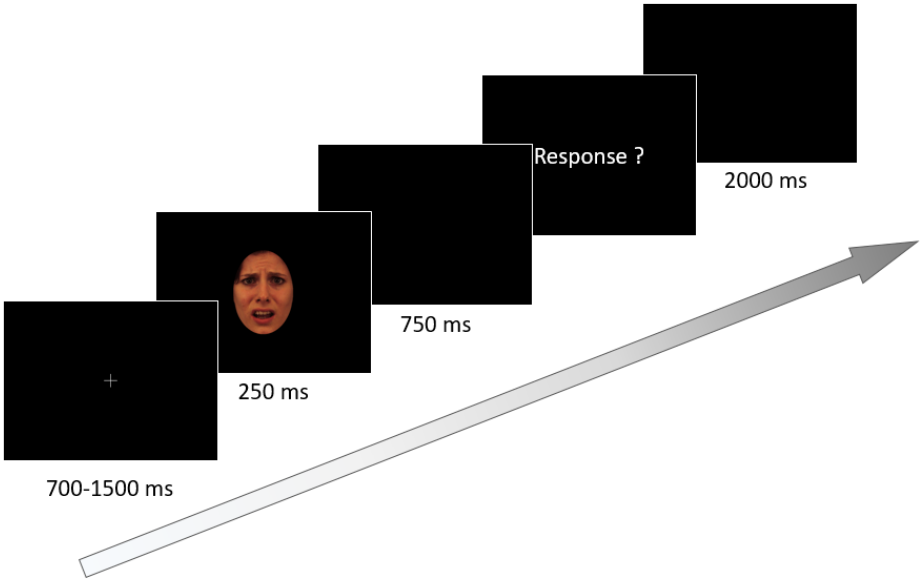

Figure 1. *At the beginning of each trial, a central fixation cross was displayed for 700-1500 ms. Then, the stimulus (male/female displaying neutral or fearful expression) appeared for 250 ms. After 750 ms the patients were prompted to respond. After the response, a black screen was displayed for 2000 ms before the start of the following trial.*

Subjects were seated comfortably in a quiet room in front of a 23'' computer screen. Stimuli were displayed using E-prime 2.0 Professional edition software (Psychology Software Tools Inc, Sharpsburg, PA, USA). Each trial began with a fixation cross displayed in the center of the screen for a pseudorandomized duration of 700-1500 ms. A face (either expressing a fearful or neutral expression) was then displayed for 250 ms, followed by a black screen for 750ms. Then, a black screen displaying "Response?" prompted the patient to respond and remained on the screen until a response was given. Finally, the response was followed by a 2000 ms black screen before the next trial began.

Patients were instructed to respond as accurately as possible, without any instruction related to the speed of the response. Each task (implicit/explicit) began by a training session of 20

trials (with different face stimuli than those using in the experimental session). Each task included 80 trials with an equal proportion of neutral expressions (figured by 20 male faces and 20 woman faces) and fearful expressions (figured by 20 male faces and 20 woman faces). The same faces were used for the two tasks. All participants were naïve about the purpose of the paradigm that aimed to contrast STN activity when focusing explicitly or implicitly on emotion recognition.

2.3. Recordings

All patients were studied two days after surgery, before the implantation of the subcutaneous stimulator. All tests and recordings were performed while patients were under their usual medication. STN LFPs were recorded by a g.BSamp® (g.tec Medical Engineering, Schiedlberg, Austria) biosignal amplifier connected to a PowerLab® 16/35 (ADInstruments, Dunedin, New Zealand) system. For each DBS electrode, activity was recorded bipolarly from all of two adjacent contacts, leading to 3 possible bipolar derivations per electrode: 0-1, 1-2, and 2-3. Signals were amplified and sampled at 1000 Hz, and monitored online using the Labchart® software (ADInstruments). Triggers corresponding to the task stimuli were sent by Eprime to the recording device through a parallel port.

2.4. Behavioral analyses

All behavioral data analyses were performed using R (version 4.0.2; R Core Team, 2020) implemented with the {lme4} package (Bates et al., 2015). Since no instructions relative to the speed of the response were provided to patients, we only focused behavioral analyses on responses accuracy. The effect of emotion valence (fear, neutral) and task (implicit, explicit) was studied using a mixed-model logistic regression using the *glmer*{lme4} function. Model

selection involved testing several models with emotion and task as fixed effects, and adding random intercepts for nuclei and random slopes for the task effect and emotion effect. We used the Akaike Information Criterion (AIC) for model selection. This criterion informs about the quality of the model with the lowest value indicating better quality. Thus, the model with the lowest AIC was selected. In this case, the following model was selected that used a logit link function and the bobyqa optimizer:

*Accuracy model = glmer(accuracy ~ emotion * task + (emotion|n), family = binomial(link = logit), glmerControl(optimizer = bobyqa))* (1)

Significance of fixed effects was evaluated by the *Anova*{car} function that provides p-values based on Wald chi-squared tests. We used mixed-models due to their advantages such as the ability to take all data into account, without the need to average at the subject-level, even in the case of unbalanced data; and also due to their ability to model random effects such as subjects (see Gueorguieva and Krystal, 2004). Marginal and conditional R^2 were obtained from the {MuMin} (Barton, 2009) package. The significance statistical threshold was set at $p = 0.05$.

2.5. LFP signal analyses

All preprocessing steps were carried out using the EEGLAB (Delorme and Makeig, 2004) toolbox for Matlab (The Mathworks, USA). All subsequent time-frequency analyses were performed with custom Matlab code (available at https://github.com/jduprez) based on published equations (Cohen, 2014).

2.5.1. Preprocessing

LFP signals were high-pass filtered offline at 0.5 Hz and epoched from −1 to 2s surrounding the stimulus (face) display. We deliberately used long epochs to avoid potential edge artifacts sometimes associated with wavelet convolution (see section 2.5.2). All epochs were visually inspected and manually removed in the case of excessive noise or artifacts. After preprocessing, 36(±3) trials per experimental condition were available on average. Two patients (corresponding to 4 STNs) were excluded from further analyses as a result of excessive noise, resulting in 28 usable STN datasets.

Contact pair selection was the result of a two-step procedure. First, anatomical location and CT scan showed that, for all patients, the most distal contact pair (0-1) was located in the ventral part of the STN (1.5 ± 4.2 mm lateral to the anterior-posterior commissure (AC-PC) line, −3.1 ± 1.7 mm posterior to the middle of the AC-PC line, and −5.4 ± 1.7 mm below this point) which has been preferentially associated with cognitive processing (see supplemental figure S1 for an example of electrode positioning). Second, a trial-by-trial breakdown (random selection of 25 trials, see supplemental figure S2) for the three pairs of contacts across all experimental conditions showed that activity was greater for the most distal pair of contacts (0-1), and decreased over the above pairs. Let us note that volume conduction prevents from affirming that the recordings only reflect ventral STN LFP. Consequently, all subsequent interpretations apply to the global STN region.

2.5.2. Time-frequency analyses

Complex Morlet wavelet convolution in the frequency domain was applied for time-frequency decomposition. Frequencies from 1 to 40 Hz were studied. Frequencies higher than 40 Hz were not investigated, since cognitive and emotional processing have been so far associated

mostly with frequencies up to the beta range. Convolution was performed by multiplying the Fourier transform of the LFP signal by the Fourier transform of a set of complex Morlet wavelet defined as :

$$e^{i2\pi ft}e^{t^2(2s^2)} \qquad (2)$$

and by taking the inverse fast-Fourier transform of the result. In equation (2), t is time, f is frequency ranging from 1 to 40 Hz in 50 logarithmically spaced steps. S corresponds to the width of the wavelets and is defined as:

$$n/2\pi f \qquad (3)$$

The parameter *n* is the number of cycles, which directly impacts the compromise between frequency and temporal resolution. A greater value of *n* will favor frequency resolution over temporal resolution, while a lower *n* will result in the opposite. We used a logarithmically increasing *n* from 4 to 10, thus favoring temporal resolution for lower frequencies, and frequency resolution for higher frequencies, which is indicated when one investigates condition-specific transient changes (Cohen, 2014).

Power was obtained by taking the squared magnitude of the resulting complex analytic signal (z) at each time point t :

$$power = real[z(t)]^2 + imaginary[z(t)]^2 \qquad (4)$$

In order to be able to compare conditions, a decibel transform was applied to normalize power results as follows:

$$dB\ power\ =\ 10\ \times log10(power/baseline) \qquad (5)$$

Baseline power was computed from -500 to -200 ms before stimulus onset. Average baseline power was calculated over all trials, irrespective of condition using that time-window.

Synchronization of STN oscillations across trials was also investigated by the means of inter-trial phase clustering (ITPC). This measure ranges from 0 to 1, and quantifies the similarity of phase across trials, with 0 indicating a uniform phase angle distribution and 1 indicating perfect phase clustering. ITPC was computed as follows:

$$ITPC\ =\ \frac{1}{n} \times \sum_{t=1}^{n} e^{i[\Phi_t]} \qquad (6)$$

In equation (6), *n* is the number of trials, and Φ is the phase angle at trial t. Given that all conditions did not have the same trial count, ITPC was normalized to ITPCz (in arbitrary units) in order to be able to compare conditions (see Cohen, 2014) :

$$ITPCz\ =\ n \times ITPC^2 \qquad (7)$$

In equation (7), *n* is the number of trials.

Further analyses were based on power and ITPC extracted from relevant time-frequency windows, for which selection was a two-step process. First, significant changes from baseline were investigated by permutation analyses (Maris and Oostenveld, 2007). For each subject and at each of the 1000 iterations, the time-frequency map was cut at a random point in time

and the second half was placed before the first half, thus resulting in a complete misalignment of the time of stimulus onset. This procedure resulted in a distribution of time-frequency maps under the null hypothesis that power/ITPCz was similar across time. A z-score transformation was then applied on the real power/ITPCz data by subtracting the average value under the null hypothesis, and dividing by its standard deviation. Correction for multiple comparisons was carried out using cluster-based correction. The significance threshold was set at $p = 0.05$.

After permutation testing, smaller time-frequency windows of interest were defined in significant clusters by visual inspection. Critically, we avoided circular inference by performing this selection on grand average maps. Hence, selection was blind to subject- or condition-specific changes in power/ITPCz, and was thus orthogonal to the effects investigated. Averaged power/ITPCz was extracted from these windows for further analyses.

Investigation of condition effects on power and ITPCz were performed by the mean of linear mixed models. Model selection was performed in the same way as described in section 2.4. In addition, compliance with the assumptions of normality and homogeneity of variance of the models' residuals was checked by visual inspection.

For all power and ITPCz analyses, the following model equation was selected:

*model = lmer(power[or ITPC] ~ emotion * task + (task|n), data = data)* (8)

However, for the ITPCz analysis focusing on one of the delta windows, a lower AIC was found when adding the nucleus (left or right) factor (although nucleus did not significantly impacted ITPCz after inspection of the results):

*model = lmer(ITPCz ~ emotion * task + nucleus + (task|n), data = data)* (9)

For all models, significance of fixed effects was evaluated by the *anova*{stats} function that provides p-values based on F tests. Marginal and conditional R^2 were also calculated for all models. When applicable, post-hoc tests were carried out using Tukey tests computed by the glht function of the {multcomp} package, which computes adjusted p-values using individual *z* tests (Hothorn et al., 2008). Each model significance threshold was adjusted using Bonferroni correction when multiple time-frequency windows were investigated, with p = 0.05/number of time-frequency windows.

2.6. LFP-behavior relationships

We investigated whether LFP time-frequency variables (power/ITPCz) were associated with patients' accuracy at the group level. We used the same linear mixed models methods as described in section 2.5.2, with the exception that accuracy was the dependent variable, and that power/ITPCz were considered as fixed effects as well as experimental condition. For models focusing on power, subject- and condition-averaged accuracy were used since no response-specific triggers in the signal allowed to link each epoch to its corresponding accuracy due to technical difficulties. The same procedure was followed for ITPCz, which is by nature an average metric since it quantifies clustering over all trials. In all cases, the following model was selected using the same criteria as described in section 2.4. :

*Accuracy-LFP model = lmer(accuracy ~ power[or ITPC] + emotion * task + (emo|n), data = data)* (10)

Compliance with the models' assumptions, significance of fixed effects, model evaluation, and adjustment of significance threshold were performed as described in section 2.5.2.

3. Results

Table 2: *Behavioral and LFP results showing mean (SD) accuracy rate, power and ITPCz extracted in the different time-frequency windows, according to the emotional valence of the stimulus and the type of task.*

		Fear - emotion	Neutral - emotion	Fear - gender	Neutral - gender
Behavior	Accuracy	0.91 (0.28)	0.91 (0.28)	0.88 (0.33)	0.88 (0.32)
Power (dB)	Delta 1	0.48 (1.5)	0.18 (1.4)	0.49 (2.8)	0.14 (2.1)
	Delta 2	0.56 (1.1)	0.49 (1.13)	-0.02 (2.7)	0.37 (1.5)
	Alpha-beta	-0.89 (1.8)	-0.86 (1.5)	-1.68 (2.3)	-1.7 (1.7)
ITPCz (a.u.)	Delta	138.7 (85.8)	120.9 (75.8)	167.8 (111.2)	152.1 (90.8)
	Theta	126.7 (108)	124.9 (127.7)	153.1 (137.1)	146.1 (134.4)

3.1. Behavioral results

Figure 2 presents accuracy as a function of stimulus emotional valence and task type. The accuracy rate appears to be higher for the emotion task (0.91, sd = 0.28) than the gender task (0.88, sd = 0.32), which was confirmed by a significant task effect (χ^2 = 7.03, p = 0.008; conditional R^2 = 0.15, marginal R^2 = 0.01). Conversely, valence of the emotional stimulus was

not associated with changes in accuracy (χ^2 = 0.3, p = 0.58), nor did it influence the effect of task (χ^2 = 0, p = 0.99). Overall, accuracy was higher for the emotion than the gender task.

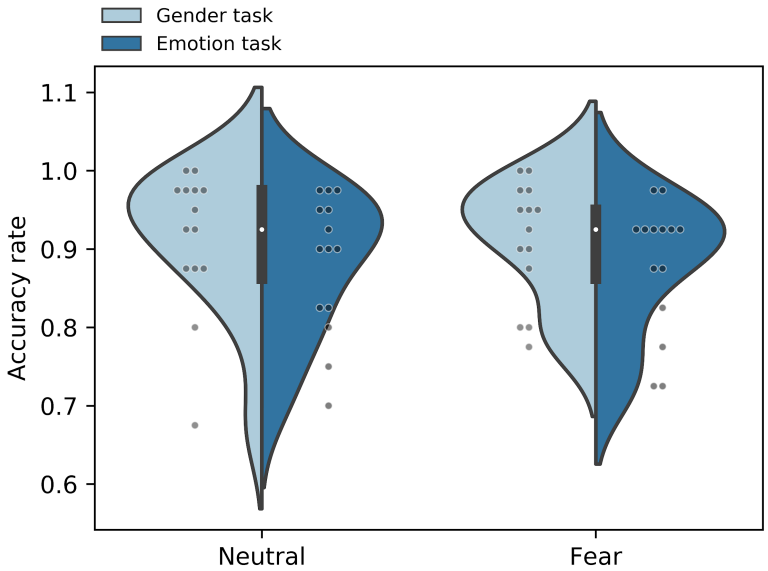

Figure 2. *Accuracy rate as a function of stimulus emotional valence and task type. Violin plots present data distribution with an inset boxplot. Each data point corresponds to the average accuracy of a subject.*

3.2. Power results

Power analyses were focused on 3 different time-frequency windows (Figure 3): 1) A first window in the "low" delta range referred to as delta 1 in the remainder of the paper (from 1.078 to 1.694 Hz, from 325 to 700 ms after stimulus onset), a second window in the "high" delta range: delta 2 (from 2.468 to 3.8774 Hz, from 295 to 655 ms), and a third window in the low-alpha-beta range (from 7.081 to 23.62 Hz, from 1465 to 1810 ms). Since we investigated three different time-frequency windows, we used a corrected significance threshold of p = 0.05/3 = 0.016.

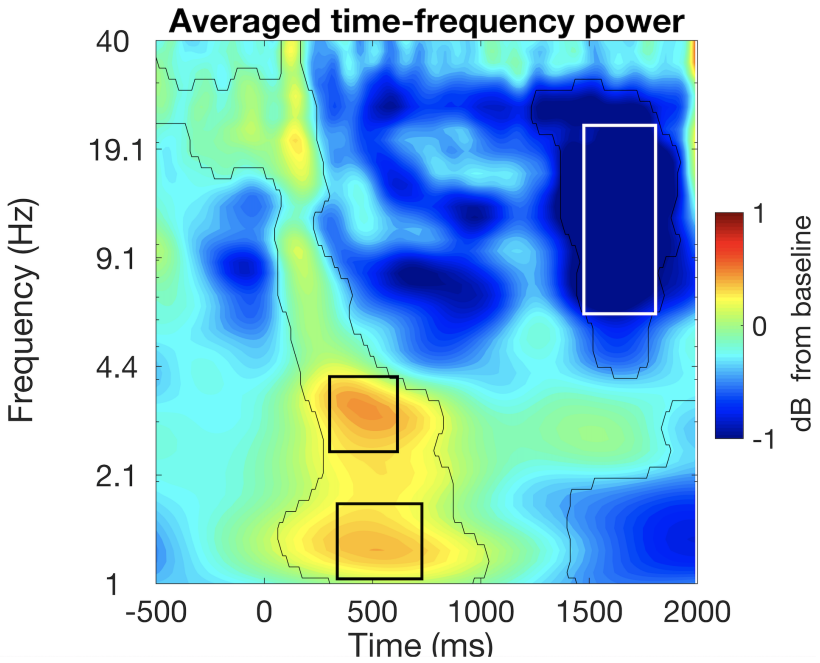

Figure 3. *Global average time-frequency power map. Time 0 corresponds to the onset of the stimulus. Black contour lines indicate the regions of significant changes from baseline after permutation analyses with cluster correction. The plain line rectangles correspond to the time-frequency windows chosen for the analyses: delta 1, delta 2, and alpha-beta band.*

3.2.1 Delta 1 window

Figure 4.A illustrates power extracted from the delta 1 time-frequency window. No clear changes in power can be observed according to either emotional valence or to task type (see also Table 2 for all condition-specific results). Statistical analyses revealed no significant effect of emotion ($F_{(1, 4060)} = 1.82$, $p = 0.18$; conditional $R^2 = 0.14$, marginal $R^2 = 0.001$), nor task ($F_{(1, 4060)} = 0.4$, $p = 0.53$), nor the interaction between the two factors ($F_{(1, 4060)} = 1.4$, $p = 0.23$).

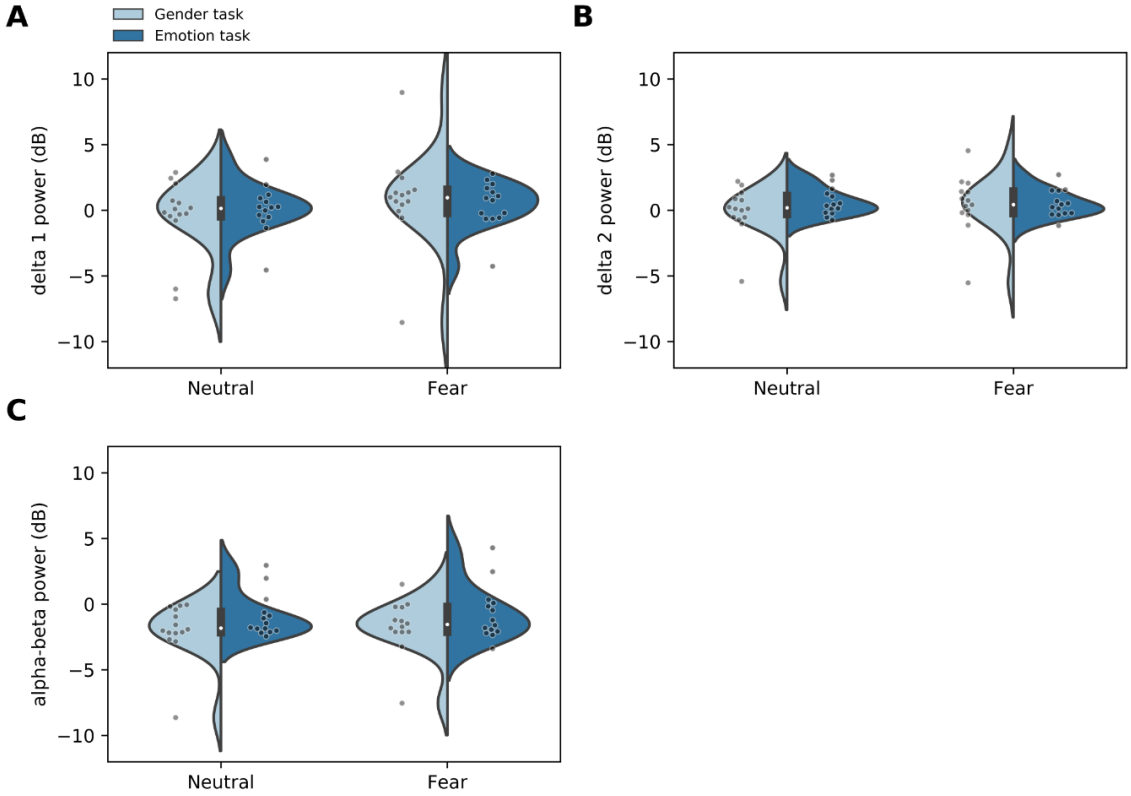

Figure 4. *Power as a function of stimulus emotional valence and task for delta 1 (A), delta 2 (B), and alpha-beta (C) time-frequency windows. Violin plots present data distribution with an inset boxplot. Each data point corresponds to the average power of a subject.*

3.2.2. Delta 2 window

Similarly to delta 1, power extracted from the delta 2 time-frequency window was similar whether the emotion displayed was neutral or fearful, or whether the task was explicit or implicit (Table 2, Figure 4.B). There was indeed no significant difference in power according to emotion ($F_{(1, 4060)} = 3.6$, $p = 0.057$; conditional $R^2 = 0.103$, marginal $R^2 = 0.005$), or task ($F_{(1, 4060)} = 0.89$, $p = 0.35$). However, we observed a significant interaction between the emotion and task factors ($F_{(1, 4060)} = 9.43$, $p = 0.002$). Post-hoc analyses revealed that delta 2 power was significantly higher for the neutral stimuli than for the fear ones during the implicit task ($p = 0.002$). All other comparisons were not significant (all $p > 0.05$).

3.2.3 Alpha-beta window

Figure 4.C presents the power extracted from the alpha-beta time-frequency window. No clear changes in power were present according to emotional valence or task in alpha beta power (Table 2), since statistical analyses revealed no significant differences between fear and neutral expressions ($F_{(1, 4060)} = 0.51$, $p = 0.47$; conditional $R^2 = 0.378$, marginal $R^2 = 0.023$), as well as between implicit and explicit task ($F_{(1, 4060)} = 3.65$, $p = 0.066$). No significant interaction was found between the two factors ($F_{(1, 4060)} = 0.25$, $p = 0.62$).

3.3. ITPCz results

ITPCz analyses focused on two different time-frequency windows. The first window was in the delta range (from 2.468 to 3.877 Hz, from 175 to 595 ms after stimulus onset), a second window was in the theta-low-alpha range (from 6.091 to 8.875 Hz, from 70 to 505 ms). Since we investigated two different time-frequency windows, we used a corrected significance threshold of $p = 0.05/2 = 0.025$.

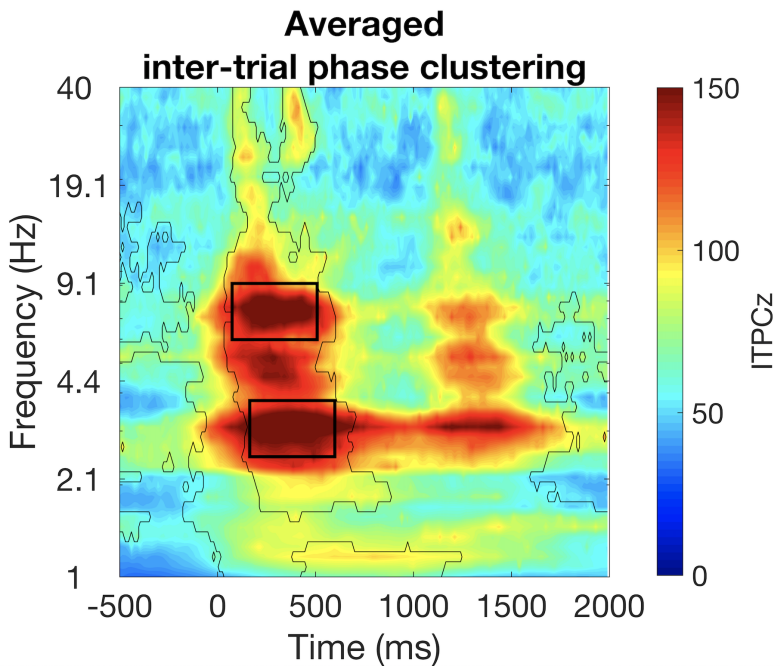

Figure 5. *Global average time-frequency ITPCz map. Time 0 corresponds to stimulus onset. Black contour lines indicate the regions of significant changes from baseline after permutation analyses with cluster correction. The plain line rectangles correspond to the time-frequency windows chosen for the analyses : delta and theta bands.*

3.3.1. Delta window

ITPCz extracted from the delta time-frequency window is presented in Figure 6.A. Although ITPCz appeared similar between the two emotional stimuli, it was greater for the implicit (160, sd = 101) than the explicit task (129.9, sd = 80.8). This was confirmed by the statistical analyses that revealed a significant task effect ($F_{(1, 81)} = 5.69$, $p = 0.024$; conditional $R^2 = 0.77$, marginal $R^2 = 0.035$), but not for emotion ($F_{(1, 81)} = 3.83$, $p = 0.055$). No significant interaction was found between task and emotion ($F_{(1, 81)} = 0.015$, $p = 0.903$). Overall, this suggests that delta phase alignment across trials was greater in the implicit than the explicit task.

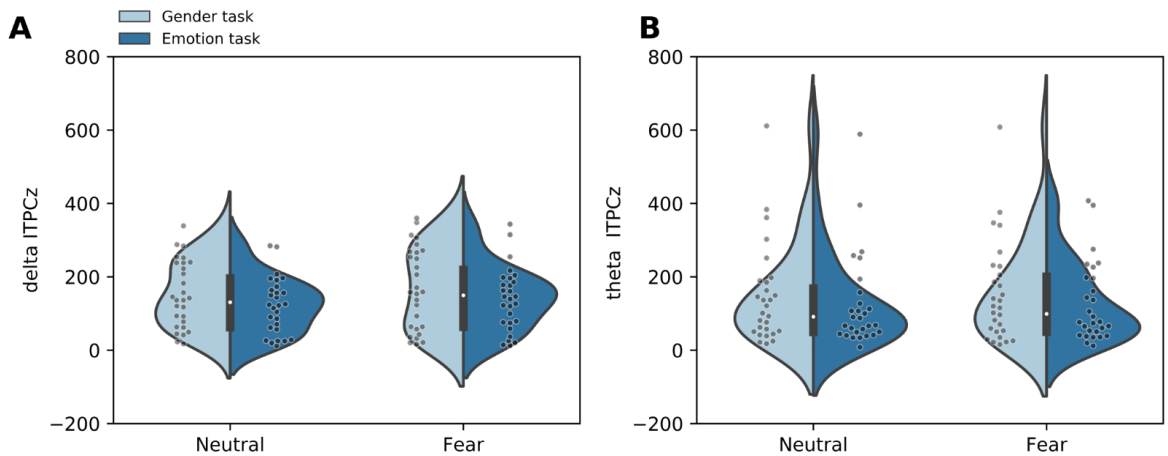

Figure 6. *ITPCz as a function of stimulus emotional valence and task type for delta (A), and theta (B) time-frequency windows. Violin plots present data distribution with an inset boxplot. Each data point corresponds to the average power of a subject.*

3.3.2. Theta window

A similar pattern of result than for delta was observed for theta ITPCz. Figure 6.B illustrates indeed that theta ITPCz appeared greater for the implicit (149.7, sd = 134.6) than the explicit (125.9, sd = 117.2) task, while no clear changes according to emotion was observed. However, the task effect was not supported by the statistical analyses, which revealed no significant difference for both task ($F_{(1, 81)} = 5.59$, $p = 0.0254$; conditional $R^2 = 0.86$, marginal $R^2 = 0.009$) and emotion effects ($F_{(1, 81)} = 0.24$, $p = 0.63$). No significant interaction was found between task and emotion effects ($F_{(1, 81)} = 0.08$, $p = 0.77$).

3.4. LFP-behavior relationships

Each power/ITPCz time-frequency window was investigated for potential association with overall accuracy at the task. Since power was extracted from three windows, and ITPCz from two windows, the same statistical significance thresholds than previously were applied: $p = 0.016$ and $p = 0.025$ for models using power and ITPCz, respectively.

We found that overall accuracy did not depend on power, whether it was extracted at delta 1 ($F_{(1, 80)} = 0.89$, $p = 0.36$; conditional $R^2 = 0.59$, marginal $R^2 = 0.04$), delta 2 ($F_{(1, 80)} = 0.46$, $p = 0.5$; conditional $R^2 = 0.59$, marginal $R^2 = 0.04$), or alpha-beta frequency ($F_{(1, 80)} = 0.16$, $p = 0.69$; conditional $R^2 = 0.59$, marginal $R^2 = 0.03$). However, a significant association was found between overall accuracy and ITPCz, since accuracy significantly depended on delta ($F_{(1, 80)} = 10.64$, $p = 0.0016$; conditional $R^2 = 0.64$, marginal $R^2 = 0.13$) and theta ITPCz ($F_{(1, 80)} = 5.89$, $p = 0.017$; conditional $R^2 = 0.72$, marginal $R^2 = 0.11$). These results indicate that stronger delta and theta ITPCz, and thus stronger phase alignment across trials, was associated with better accuracy in both delta and theta windows.

4. Discussion

Here, we aimed at characterizing the modulation of neural oscillations in response to emotional faces depending on the orientation of attentional resources using explicit (emotional categorization) and implicit (gender categorization) tasks. Considering the STN central place in motor, cognitive, and limbic functions, we expected changes in STN neural oscillatory dynamics in different frequency bands (theta, alpha and beta) in response to emotional faces in different attentional orientation situations. Finally, we expected that these changes would be associated with behavior. Our result confirmed STN involvement during facial emotion processing. Interestingly, changes in neural oscillations were associated with frequencies lower than expected (delta-theta), and were more important for phase synchronization than power.

4.1. Accuracy depends on the nature of task

In order to evaluate STN involvement in explicit and implicit emotional processing, we relied on a task that puts the participant in two different attentional situations: they were asked to either discriminate between two facial emotions (explicit task), or to recognize face gender (implicit task). In both situations, facial emotion could vary between neutral faces and fear-expressing faces. Patients in our study were equally accurate whether the faces expressed fear or a neutral expression. However, patients were less accurate when they had to focus on the non-emotional attribute of the stimulus (gender). These results could be interpreted as the consequence of an interfering effect of emotional stimuli on gender categorization, which would be in line with previous observations proposing that the saliency of emotional faces

could capture attention (Carretié, 2014; Cohen et al., 2016). However, the absence of an emotional valence effect on behavior in our study mitigates this interpretation. Nonetheless, we cannot rule out the possibility that categorizing gender could have been made more difficult by the presence of varying emotional expressions throughout the task. Another way to interpret these results could be that the gender categorization task was inherently more difficult because of the absence of non-facial features such as hair. These attributes are less relevant for the discrimination of facial expression.

We did not observe lower accuracy for fear compared to neutral expressions in the implicit task, which was reported by Knyazev et al. (2009). This discrepancy is hard to explain, since studies using such tasks are scarce. One possible explanation is that accuracy in our study was not evaluated in the same way for both explicit and implicit tasks. Indeed, in Knyazev et al. (2009), accuracy in the explicit task was dissociated from gender categorization and participants were asked to judge the friendliness of the face instead of a simple emotion categorization. Overall, our results suggest that behavioral performances during the task were more affected by the nature of the task than by stimuli emotional valence.

4.2. Emotional valence is associated with STN low frequency power

Enhancement in beta oscillations' power is mostly associated with motor behavior, and is considered to be a neurophysiologic marker of PD related to rigidity and bradykinesia. Nevertheless, beta oscillations were also involved in orienting attentional resources (Buschman and Miller, 2007) and have been suggested to play a role in active inhibition in cognitive and motor contexts (Zavala et al., 2015). Other frequency bands have been

associated with cognitive processing in the STN, such as the theta band that has been repeatedly reported to be involved in conflict processing (Cavanagh et al., 2011; Duprez et al., 2019). Regarding emotional stimuli processing, changes in STN oscillatory power were mostly described in the alpha band (Brücke et al., 2007; Huebl et al., 2014). Changes in alpha band power according to emotional processing has also been described for vocal emotional stimuli (Benis et al., 2020). Consequently, we expected changes in STN power for the alpha band, since our task was designed to induce explicit and implicit emotional processing by the STN. Our results illustrate a clear increase in delta power around 500 ms after stimulus presentation, and an alpha-beta decrease around 1500 ms, so around 500 ms after that the patients were prompted to respond. We found a greater increase in delta power for neutral as compared to fear-expressing faces, but only in the implicit condition, advocating for STN involvement in implicit emotional processing. However, we did not observe any power modulations in theta, alpha and beta bands by either stimulus emotional valence of the stimulus, or by the task nature, i.e. whether emotion processing was explicit or implicit. Furthermore, we did not identify any relationship between STN power at the investigated frequencies and patients' behavioral performances (overall accuracy). On the one hand, absence of alpha-beta power modulations by emotional valence or attention focus is surprising, since changes in alpha power have been associated with the processing of pleasant, as compared to unpleasant stimuli. One possible interpretation of this discrepancy is the presence of differences in task design. For instance, we chose to focus only on unpleasant (fear expression) and neutral stimuli. Furthermore, our task involved an active discrimination behavior (valence or gender), while previous STN-LFP studies reporting alpha changes used passive viewing paradigms (Brücke et al., 2007; Huebl et al., 2014; Kühn et al., 2005), with stimuli remaining on the screen for 1-2 s. Hence, our task involved further

cognitive processing and motor behavior. On the other hand, this implicit/explicit task, which necessarily involves a complex interaction between emotional processing, orientation of attention, and cognitive control, has never been performed before with STN-LFP recordings (although it has been with EEG (Yu et al., 2014)). Consequently, the interaction of emotion-, attention-, or cognitive control-specific STN oscillatory changes would hardly be seen as a simple combination of all previously known dynamics.

4.3. STN functional organization changes with emotional valence and attentional focus and is associated with behavior

Most studies investigating STN-LFP neural oscillations focus on power results extracted from time-frequency decomposition methods. Aside from a few exceptions (Duprez et al., 2019; Zavala et al., 2016, 2013), phase information of STN oscillations is either ignored or not reported. However, neural oscillatory phase carries valuable information, especially when studying how phase is consistent across trials of an experiment. Here, we investigated inter-trial phase clustering (ITPC), which can be mathematically defined as the strength with which the timing of frequency-specific oscillations clusters over trials. This can be interpreted as an index of functional organization, since strong clustering indicates that oscillations have a similar timing across trials (Cohen, 2014). Our results showed a transient increase in functional organization occuring around 300 ms after stimulus presentation in the delta and theta bands, indicating that organization of delta and theta oscillations became temporarily consistent across trials. Although insensitive to the valence of facial emotion, delta functional organization depended on whether the task was explicit or implicit, with stronger functional organization for the implicit task. It is worth noting that the time-frequency window with

increased delta ITPC coincides with the window for power increase that we described as high delta. No task-related changes were observed for theta oscillations. Furthermore, we provided evidence that delta and theta functional organization are linked with behavioral performance, since an increase in phase clustering was associated with greater tasks' accuracy. Taken together, our results suggest that delta and theta functional organization in the STN are involved in both the implicit and explicit tasks, and even more strongly for the implicit task. It is interesting to note that delta oscillation modulations in the STN have been reported in situations of cognitive control (Zavala et al., 2013). This was also described at the cortical level in EEG studies, especially during errors (Cohen and van Gaal, 2014). Cortical delta oscillations were also proposed to be associated with attention, especially while detecting relevant stimuli when distractors are present (Herrmann et al., 2016). Although it is hazardous to directly compare cortical and STN delta oscillations, the greater delta ITPC increase that was observed in our study for the implicit task as compared to the explicit task could be interpreted as a result of a greater need for cognitive control. Indeed, the implicit task was associated with lower accuracy and seemed more difficult. As argued in section 4.1, this greater cognitive demand could arise from an interference of emotional information with the gender categorization of the task (Carretié, 2014), however the influence of the absence of non-facial features cannot not be excluded.

4.4. Limitations

A first limitation to our study is the small sample of patients (n = 16). Small samples are however inherent to human LFP studies, given the recruitment difficulties associated with the low number of patients that can undergo STN DBS. Nevertheless, larger samples would lead

to more robust and generalizable findings. Second, the influence of dopaminergic medication on STN oscillatory activity in emotional processes has to be clarified in further studies. Indeed, based on the levodopa equivalent daily dose standard deviation, the variability in dopaminergic medication was rather high in our sample. However, this dosage does not reflect an optimized postoperative dopaminergic status and would not allow for a proper control given that the oral treatments are inevitably being optimized during the postoperative period. In this regard, being able to record LFP after treatment optimization would be very helpful. Although such recordings are difficult with current setups, future stimulator technologies will help resolve this issue. Another issue concerns the association between STN activity and behavior. Indeed, due to technical difficulties, the signal had no response-specific triggers, which prevented an evaluation of the effect of power on accuracy at the trial-level, thus diminishing power. Furthermore, regarding task design, only one negative emotional valence was used in this study (to maximize the number of trials per condition). Thus, we cannot extend the discussion further on the effect of emotional valence that was found in others studies using positive and negative valences.

5. Conclusion

A growing body of literature confirms that the STN is not exclusively a motor territory, but has also an integrative role for cognitive and limbic processes which constantly interact to give rise to the adapted behavior. Our study shows for the first time that the STN is involved in emotional processing, even when emotional information is not relevant to the situation, and attention is directed toward non-emotional stimuli characteristics. Our study shows that delta and theta oscillations, which are both involved in cognitive control, appear to play an

important role in explicit and implicit emotional processing, and are associated with behavior. Interestingly, these results were stronger for STN oscillations phase synchronization than for power. We interpret these findings of delta and theta oscillatory changes and association with behavior as reflecting a greater need for cognitive control.

6. References

Barton, K., 2009. MuMIn: multi-model inference. http://r-forge. r-project. org/projects/mumin/.

Bates, D., Mächler, M., Bolker, B., Walker, S., 2015. Fitting Linear Mixed-Effects Models Using lme4. Journal of Statistical Software 67, 1–48. https://doi.org/10.18637/jss.v067.i01

Benis, D., Haegelen, C., Voruz, P., Pierce, J., Milesi, V., Houvenaghel, J.-F., Vérin, M., Sauleau, P., Grandjean, D., Péron, J., 2020. Subthalamic nucleus oscillations during vocal emotion processing are dependent of the motor asymmetry of Parkinson's disease. NeuroImage 222, 117215. https://doi.org/10.1016/j.neuroimage.2020.117215

Benton, A.L., Abigail, B., Sivan, A.B., Hamsher, K. deS, Varney, N.R., Spreen, O., 1994. Contributions to neuropsychological assessment: A clinical manual. Oxford University Press, USA.

Biseul, I., Sauleau, P., Haegelen, C., Trebon, P., Drapier, D., Raoul, S., Drapier, S., Lallement, F., Rivier, I., Lajat, Y., Verin, M., 2005. Fear recognition is impaired by subthalamic nucleus stimulation in Parkinson's disease. Neuropsychologia 43, 1054–1059. https://doi.org/10.1016/j.neuropsychologia.2004.10.006

Brücke, C., Kupsch, A., Schneider, G.-H., Hariz, M.I., Nuttin, B., Kopp, U., Kempf, F., Trottenberg, T., Doyle, L., Chen, C.C., Yarrow, K., Brown, P., Kühn, A.A., 2007. The subthalamic region is activated during valence-related emotional processing in patients with Parkinson's disease. Eur. J. Neurosci. 26, 767–774. https://doi.org/10.1111/j.1460-9568.2007.05683.x

Buschman, T.J., Miller, E.K., 2007. Top-down versus bottom-up control of attention in the prefrontal and posterior parietal cortices. Science 315, 1860–1862. https://doi.org/10.1126/science.1138071

Carretié, L., 2014. Exogenous (automatic) attention to emotional stimuli: a review. Cogn Affect Behav Neurosci 14, 1228–1258. https://doi.org/10.3758/s13415-014-0270-2

Cavanagh, J.F., Wiecki, T.V., Cohen, M.X., Figueroa, C.M., Samanta, J., Sherman, S.J., Frank, M.J., 2011. Subthalamic nucleus stimulation reverses mediofrontal influence over decision threshold. Nat. Neurosci. 14, 1462–1467. https://doi.org/10.1038/nn.2925

Cohen, M.X., 2014. Analyzing neural time series data: theory and practice. MIT press.

Cohen, M.X., van Gaal, S., 2014. Subthreshold muscle twitches dissociate oscillatory neural signatures of conflicts from errors. Neuroimage 86, 503–513. https://doi.org/10.1016/j.neuroimage.2013.10.033

Cohen, N., Moyal, N., Lichtenstein-Vidne, L., Henik, A., 2016. Explicit vs. implicit emotional processing: The interaction between processing type and executive control. Cogn Emot 30, 325–339. https://doi.org/10.1080/02699931.2014.1000830

Delorme, A., Makeig, S., 2004. EEGLAB: an open source toolbox for analysis of single-trial EEG dynamics including independent component analysis. J. Neurosci. Methods 134, 9–21. https://doi.org/10.1016/j.jneumeth.2003.10.009

Delplanque, S., N'diaye, K., Scherer, K., Grandjean, D., 2007. Spatial frequencies or emotional effects?: A systematic measure of spatial frequencies for IAPS pictures by a discrete wavelet analysis. Journal of Neuroscience Methods 165, 144–150. https://doi.org/10.1016/j.jneumeth.2007.05.030

Dolan, R.J., 2002. Emotion, cognition, and behavior. Science 298, 1191–1194. https://doi.org/10.1126/science.1076358

Drapier, D., Péron, J., Leray, E., Sauleau, P., Biseul, I., Drapier, S., Le Jeune, F., Travers, D., Bourguignon, A., Haegelen, C., Millet, B., Vérin, M., 2008. Emotion recognition impairment and apathy after subthalamic nucleus stimulation in Parkinson's disease have separate neural substrates. Neuropsychologia 46, 2796–2801.

https://doi.org/10.1016/j.neuropsychologia.2008.05.006
Dujardin, K., Blairy, S., Defebvre, L., Krystkowiak, P., Hess, U., Blond, S., Destee, A., 2004. Subthalamic nucleus stimulation induces deficits in decoding emotional facial expressions in Parkinson's disease. Journal of Neurology, Neurosurgery & Psychiatry 75, 202–208.
Duprez, J., Houvenaghel, J.-F., Dondaine, T., Péron, J., Haegelen, C., Drapier, S., Modolo, J., Jannin, P., Vérin, M., Sauleau, P., 2019. Subthalamic nucleus local field potentials recordings reveal subtle effects of promised reward during conflict resolution in Parkinson's disease. Neuroimage 197, 232–242. https://doi.org/10.1016/j.neuroimage.2019.04.071
Elgebaly, A., Elfil, M., Attia, A., Magdy, M., Negida, A., 2018. Neuropsychological performance changes following subthalamic versus pallidal deep brain stimulation in Parkinson's disease: a systematic review and metaanalysis. CNS Spectr 23, 10–23. https://doi.org/10.1017/S1092852917000062
Engel, A.K., Fries, P., 2010. Beta-band oscillations--signalling the status quo? Curr. Opin. Neurobiol. 20, 156–165. https://doi.org/10.1016/j.conb.2010.02.015
Gueorguieva, R., Krystal, J.H., 2004. Move over ANOVA: progress in analyzing repeated-measures data and its reflection in papers published in the Archives of General Psychiatry. Arch. Gen. Psychiatry 61, 310–317. https://doi.org/10.1001/archpsyc.61.3.310
Herrmann, C.S., Strüber, D., Helfrich, R.F., Engel, A.K., 2016. EEG oscillations: From correlation to causality. International Journal of Psychophysiology, Research on Brain Oscillations and Connectivity in A New Take-Off State 103, 12–21. https://doi.org/10.1016/j.ijpsycho.2015.02.003
Hothorn, T., Bretz, F., Westfall, P., 2008. Simultaneous Inference in General Parametric Models. Biometrical Journal 50, 346–363.
Huebl, J., Schoenecker, T., Siegert, S., Brücke, C., Schneider, G.-H., Kupsch, A., Yarrow, K., Kühn, A.A., 2011. Modulation of subthalamic alpha activity to emotional stimuli correlates with depressive symptoms in Parkinson's disease. Mov. Disord. 26, 477–483. https://doi.org/10.1002/mds.23515
Huebl, J., Spitzer, B., Brücke, C., Schönecker, T., Kupsch, A., Alesch, F., Schneider, G.-H., Kühn, A.A., 2014. Oscillatory subthalamic nucleus activity is modulated by dopamine during emotional processing in Parkinson's disease. Cortex 60, 69–81. https://doi.org/10.1016/j.cortex.2014.02.019
Knyazev, G.G., Slobodskoj-Plusnin, J.Y., Bocharov, A.V., 2009. Event-related delta and theta synchronization during explicit and implicit emotion processing. Neuroscience 164, 1588–1600. https://doi.org/10.1016/j.neuroscience.2009.09.057
Kühn, A.A., Hariz, M.I., Silberstein, P., Tisch, S., Kupsch, A., Schneider, G.-H., Limousin-Dowsey, P., Yarrow, K., Brown, P., 2005. Activation of the subthalamic region during emotional processing in Parkinson disease. Neurology 65, 707–713.
Little, S., Brown, P., 2014. The functional role of beta oscillations in Parkinson's disease. Parkinsonism Relat. Disord. 20 Suppl 1, S44-48. https://doi.org/10.1016/S1353-8020(13)70013-0
Lundqvist, D., Flykt, A., Öhman, A., 1998. The Karolinska directed emotional faces (KDEF). CD ROM from Department of Clinical Neuroscience, Psychology section, Karolinska Institutet 91, 2–2.
Maris, E., Oostenveld, R., 2007. Nonparametric statistical testing of EEG- and MEG-data. J. Neurosci. Methods 164, 177–190. https://doi.org/10.1016/j.jneumeth.2007.03.024
Ochsner, K.N., Phelps, E., 2007. Emerging perspectives on emotion-cognition interactions. Trends Cogn. Sci. (Regul. Ed.) 11, 317–318. https://doi.org/10.1016/j.tics.2007.06.008
Odekerken, V.J.J., Boel, J.A., Geurtsen, G.J., Schmand, B.A., Dekker, I.P., de Haan, R.J., Schuurman, P.R., de Bie, R.M.A., NSTAPS Study Group, 2015. Neuropsychological outcome after deep brain stimulation for Parkinson disease. Neurology 84, 1355–1361. https://doi.org/10.1212/WNL.0000000000001419

Péron, J., Dondaine, T., Le Jeune, F., Grandjean, D., Vérin, M., 2012. Emotional processing in Parkinson's disease: a systematic review. Movement Disorders 27, 186–199.

Péron, J., Renaud, O., Haegelen, C., Tamarit, L., Milesi, V., Houvenaghel, J.-F., Dondaine, T., Vérin, M., Sauleau, P., Grandjean, D., 2017. Vocal emotion decoding in the subthalamic nucleus: An intracranial ERP study in Parkinson's disease. Brain Lang 168, 1–11. https://doi.org/10.1016/j.bandl.2016.12.003

Pessoa, L., 2008. On the relationship between emotion and cognition. Nat. Rev. Neurosci. 9, 148–158. https://doi.org/10.1038/nrn2317

Plantinga, B.R., Temel, Y., Duchin, Y., Uludağ, K., Patriat, R., Roebroeck, A., Kuijf, M., Jahanshahi, A., Romenij, B. ter H., Vitek, J., Harel, N., 2018. Individualized parcellation of the subthalamic nucleus in patients with Parkinson's disease with 7T MRI. Neuroimage 168, 403–411. https://doi.org/10.1016/j.neuroimage.2016.09.023

R Core Team, 2020. R: A Language and Environment for Statistical Computing. R Foundation for Statistical Computing, Vienna, Austria.

Schroeder, U., Kuehler, A., Hennenlotter, A., Haslinger, B., Tronnier, V.M., Krause, M., Pfister, R., Sprengelmeyer, R., Lange, K.W., Ceballos-Baumann, A.O., 2004. Facial expression recognition and subthalamic nucleus stimulation. J. Neurol. Neurosurg. Psychiatry 75, 648–650. https://doi.org/10.1136/jnnp.2003.019794

Sieger, T., Serranová, T., Růžička, F., Vostatek, P., Wild, J., Štastná, D., Bonnet, C., Novák, D., Růžička, E., Urgošík, D., Jech, R., 2015. Distinct populations of neurons respond to emotional valence and arousal in the human subthalamic nucleus. Proc. Natl. Acad. Sci. U.S.A. 112, 3116–3121. https://doi.org/10.1073/pnas.1410709112

Welter, M.L., Houeto, J.L., Tezenas du Montcel, S., Mesnage, V., Bonnet, A.M., Pillon, B., Arnulf, I., Pidoux, B., Dormont, D., Cornu, P., Agid, Y., 2002. Clinical predictive factors of subthalamic stimulation in Parkinson's disease. Brain 125, 575–583.

Yu, F., Ye, R., Sun, S., Carretié, L., Zhang, L., Dong, Y., Zhu, C., Luo, Y., Wang, K., 2014. Dissociation of Neural Substrates of Response Inhibition to Negative Information between Implicit and Explicit Facial Go/Nogo Tasks: Evidence from an Electrophysiological Study. PLoS ONE 9. https://doi.org/10.1371/journal.pone.0109839

Zavala, B., Brittain, J.-S., Jenkinson, N., Ashkan, K., Foltynie, T., Limousin, P., Zrinzo, L., Green, A.L., Aziz, T., Zaghloul, K., Brown, P., 2013. Subthalamic Nucleus Local Field Potential Activity during the Eriksen Flanker Task Reveals a Novel Role for Theta Phase during Conflict Monitoring. J. Neurosci. 33, 14758–14766. https://doi.org/10.1523/JNEUROSCI.1036-13.2013

Zavala, B., Tan, H., Ashkan, K., Foltynie, T., Limousin, P., Zrinzo, L., Zaghloul, K., Brown, P., 2016. Human subthalamic nucleus–medial frontal cortex theta phase coherence is involved in conflict and error related cortical monitoring. NeuroImage 137, 178–187. https://doi.org/10.1016/j.neuroimage.2016.05.031

Zavala, B., Zaghloul, K., Brown, P., 2015. The subthalamic nucleus, oscillations, and conflict. Movement Disorders 30, 328–338. https://doi.org/10.1002/mds.26072

7. Supplemental materials

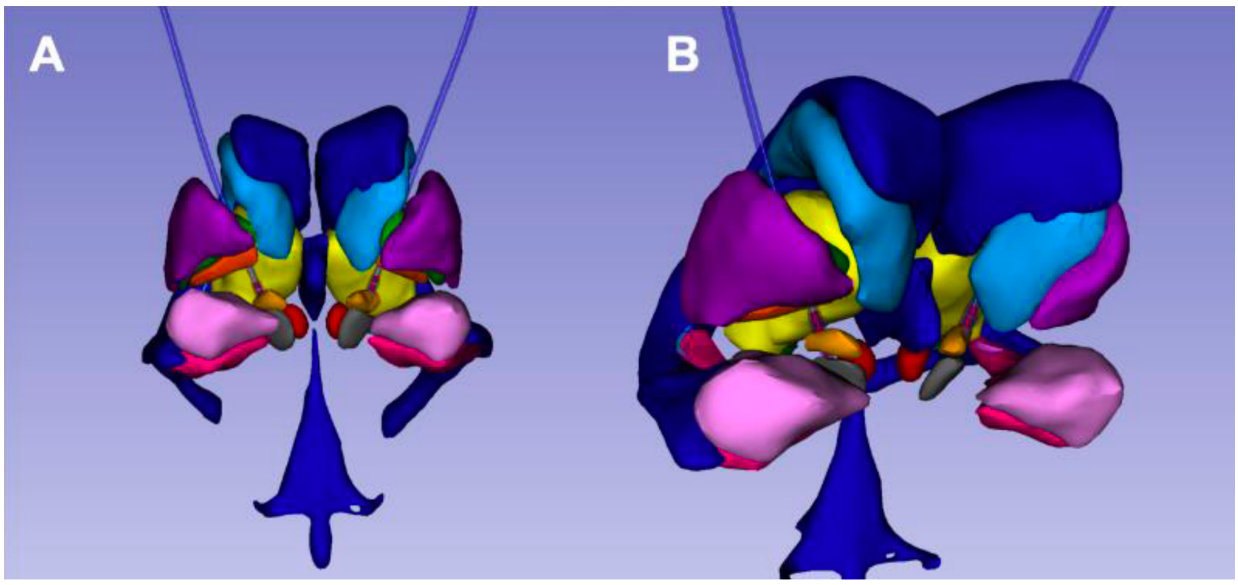

S1. Atlas-based reconstruction showing electrode and contacts position in one patient with the more distal contacts located in the STN (in orange).

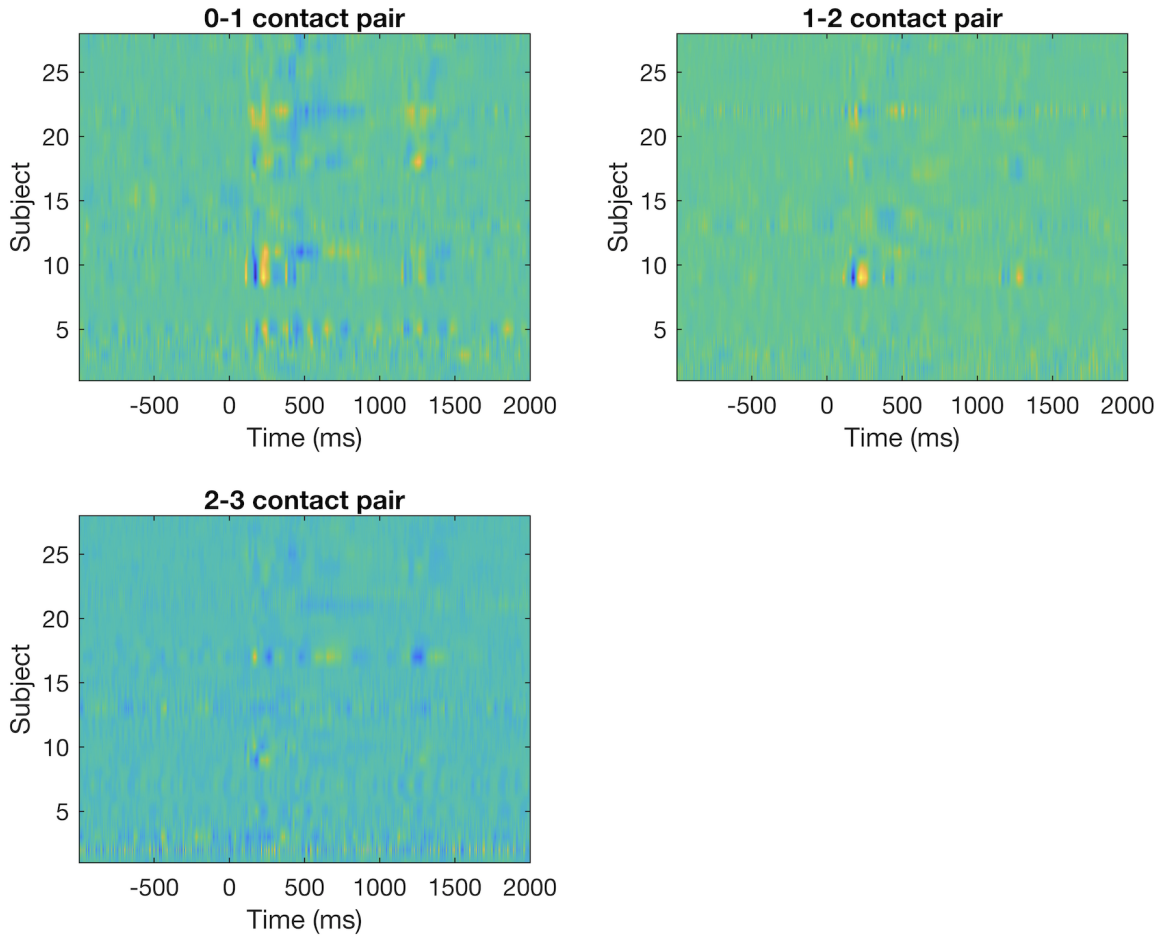

S2. Group-level ERP breakdown of intracranial recordings (ERP computed on all trials) in distal (0-1), intermediate (1-2) and proximal (2-3) pairs of contacts. The marked activity in the distal pair decreased in the intermediate pair of contacts and was merely visible on the proximal pair of contacts. Time 0 represents stimulus onset.